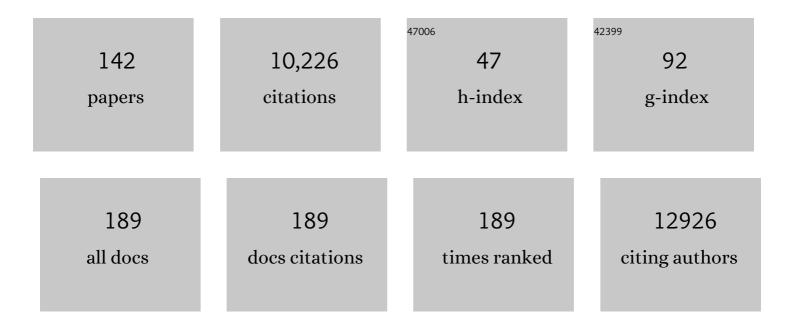
List of Publications by Year in descending order

Source: https://exaly.com/author-pdf/2094773/publications.pdf Version: 2024-02-01



#	Article	IF	CITATIONS
1	Structure of a bacterial Rhs effector exported by the type VI secretion system. PLoS Pathogens, 2022, 18, e1010182.	4.7	24
2	Structure of the Mon1-Ccz1 complex reveals molecular basis of membrane binding for Rab7 activation. Proceedings of the National Academy of Sciences of the United States of America, 2022, 119, .	7.1	12
3	Structures from intact myofibrils reveal mechanism of thin filament regulation through nebulin. Science, 2022, 375, eabn1934.	12.6	69
4	Recent developments in automated single-particle selection. Nature Reviews Methods Primers, 2022, 2,	21.2	2
5	Neutralizing antibody responses 300 days after SARSâ€CoVâ€2 infection and induction of high antibody titers after vaccination. European Journal of Immunology, 2022, 52, 810-815.	2.9	9
6	Structure of the RZZ complex and molecular basis of Spindlyâ€driven corona assembly at human kinetochores. EMBO Journal, 2022, 41, e110411.	7.8	20
7	Structure of the human inner kinetochore CCAN complex and its significance for human centromere organization. Molecular Cell, 2022, 82, 2113-2131.e8.	9.7	37
8	Cryo‣M Resolves Molecular Recognition Of An Optojasp Photoswitch Bound To Actin Filaments In Both Switch States. Angewandte Chemie - International Edition, 2021, 60, 8678-8682.	13.8	20
9	Cryoâ€EM Resolves Molecular Recognition Of An Optojasp Photoswitch Bound To Actin Filaments In Both Switch States. Angewandte Chemie, 2021, 133, 8760-8764.	2.0	4
10	The molecular basis for sarcomere organization in vertebrate skeletal muscle. Cell, 2021, 184, 2135-2150.e13.	28.9	99
11	Towards DNAâ€Encoded Micellar Chemistry: DNAâ€Micelle Association and Environment Sensitivity of Catalysis. Chemistry - A European Journal, 2021, 27, 10048-10057.	3.3	8
12	Fluorescence-guided lamella fabrication with ENZEL, an integrated cryogenic CLEM solution for the cryo-electron tomography workflow. Microscopy and Microanalysis, 2021, 27, 3234-3235.	0.4	1
13	The molecular basis for sarcomere organization in vertebrate skeletal muscle. Microscopy and Microanalysis, 2021, 27, 2832-2835.	0.4	1
14	Structural basis of human separase regulation by securin and CDK1–cyclin B1. Nature, 2021, 596, 138-142.	27.8	51
15	ENZEL - A cryogenic, retrofittable, coincident fluorescence, electron, and ion beam solution for the cryo-electron tomography workflow Microscopy and Microanalysis, 2021, 27, 3228-3229.	0.4	2
16	Remodeling of the Fibrillation Pathway of α‣ynuclein by Interaction with Antimicrobial Peptide LLâ€III. Chemistry - A European Journal, 2021, 27, 11845-11851.	3.3	12
17	New hardware for a streamlined cryo focused ion beam milling workflow. Microscopy and Microanalysis, 2021, 27, 2082-2086.	0.4	0
18	TSC1 binding to lysosomal PIPs is required for TSC complex translocation and mTORC1 regulation. Molecular Cell, 2021, 81, 2705-2721.e8.	9.7	25

#	Article	IF	CITATIONS
19	A streamlined workflow for automated cryo focused ion beam milling. Journal of Structural Biology, 2021, 213, 107743.	2.8	60
20	A barbed end interference mechanism reveals how capping protein promotes nucleation in branched actin networks. Nature Communications, 2021, 12, 5329.	12.8	57
21	Flexible open conformation of the AP-3 complex explains its role in cargo recruitment at the Golgi. Journal of Biological Chemistry, 2021, 297, 101334.	3.4	8
22	Mechanism of actin-dependent activation of nucleotidyl cyclase toxins from bacterial human pathogens. Nature Communications, 2021, 12, 6628.	12.8	13
23	Molecular architecture of black widow spider neurotoxins. Nature Communications, 2021, 12, 6956.	12.8	4
24	High-resolution structures of the actomyosin-V complex in three nucleotide states provide insights into the force generation mechanism. ELife, 2021, 10, .	6.0	27
25	Small molecule modulation of the Drosophila Slo channel elucidated by cryo-EM. Nature Communications, 2021, 12, 7164.	12.8	9
26	Towards a structural understanding of the remodeling of the actin cytoskeleton. Seminars in Cell and Developmental Biology, 2020, 102, 51-64.	5.0	63
27	Cryo-EM structure of the fully-loaded asymmetric anthrax lethal toxin in its heptameric pre-pore state. PLoS Pathogens, 2020, 16, e1008530.	4.7	17
28	TranSPHIRE: automated and feedback-optimized on-the-fly processing for cryo-EM. Nature Communications, 2020, 11, 5716.	12.8	60
29	Glycan-dependent cell adhesion mechanism of Tc toxins. Nature Communications, 2020, 11, 2694.	12.8	24
30	Structural Effects and Functional Implications of Phalloidin and Jasplakinolide Binding to Actin Filaments. Structure, 2020, 28, 437-449.e5.	3.3	83
31	The evolution of SPHIRE-crYOLO particle picking and its application in automated cryo-EM processing workflows. Communications Biology, 2020, 3, 61.	4.4	49
32	Two particle-picking procedures for filamentous proteins: <i>SPHIRE-crYOLO</i> filament mode and <i>SPHIRE-STRIPER</i> . Acta Crystallographica Section D: Structural Biology, 2020, 76, 613-620.	2.3	46
33	Structure of the Lifeact–F-actin complex. PLoS Biology, 2020, 18, e3000925.	5.6	40
34	Structure of the human BBSome core complex. ELife, 2020, 9, .	6.0	59
35	Structural basis of TRPC4 regulation by calmodulin and pharmacological agents. ELife, 2020, 9, .	6.0	38
36	Structural basis for effector transmembrane domain recognition by type VI secretion system chaperones. ELife, 2020, 9, .	6.0	26

#	Article	IF	CITATIONS
37	Structure of the Lifeact–F-actin complex. , 2020, 18, e3000925.		Ο
38	Structure of the Lifeact–F-actin complex. , 2020, 18, e3000925.		0
39	Structure of the Lifeact–F-actin complex. , 2020, 18, e3000925.		Ο
40	Structure of the Lifeact–F-actin complex. , 2020, 18, e3000925.		0
41	Structure of the Lifeact–F-actin complex. , 2020, 18, e3000925.		0
42	Structure of the Lifeact–F-actin complex. , 2020, 18, e3000925.		0
43	Title is missing!. , 2020, 16, e1008530.		0
44	Title is missing!. , 2020, 16, e1008530.		0
45	Title is missing!. , 2020, 16, e1008530.		0
46	Title is missing!. , 2020, 16, e1008530.		0
47	Reconstitution of recombinant human CCR4-NOT reveals molecular insights into regulated deadenylation. Nature Communications, 2019, 10, 3173.	12.8	65
48	Common architecture of Tc toxins from human and insect pathogenic bacteria. Science Advances, 2019, 5, eaax6497.	10.3	29
49	Structure of a Tc holotoxin pore provides insights into the translocation mechanism. Proceedings of the United States of America, 2019, 116, 23083-23090.	7.1	32
50	Cryo-EM structure of the ClpXP protein degradation machinery. Nature Structural and Molecular Biology, 2019, 26, 946-954.	8.2	68
51	Big insights from tiny crystals. Nature Chemistry, 2019, 11, 106-108.	13.6	5
52	SPHIRE-crYOLO is a fast and accurate fully automated particle picker for cryo-EM. Communications Biology, 2019, 2, 218.	4.4	860
53	Micellar BrÃ,nsted Acid Mediated Synthesis of DNA-Tagged Heterocycles. Journal of the American Chemical Society, 2019, 141, 10546-10555.	13.7	59
54	Tc Toxin Complexes: Assembly, Membrane Permeation, and Protein Translocation. Annual Review of Microbiology, 2019, 73, 247-265.	7.3	36

#	Article	IF	CITATIONS
55	Towards the application of Tc toxins as a universal protein translocation system. Nature Communications, 2019, 10, 5263.	12.8	27
56	Cryo-EM reveals the asymmetric assembly of squid hemocyanin. IUCrJ, 2019, 6, 426-437.	2.2	7
57	Profilin and formin constitute a pacemaker system for robust actin filament growth. ELife, 2019, 8, .	6.0	80
58	Arrest of trans-SNARE zippering uncovers loosely and tightly docked intermediates in membrane fusion. Journal of Biological Chemistry, 2018, 293, 8645-8655.	3.4	26
59	The complex simplicity of the bacterial cytoskeleton. Proceedings of the National Academy of Sciences of the United States of America, 2018, 115, 3205-3206.	7.1	Ο
60	Precipitation with polyethylene glycol followed by washing and pelleting by ultracentrifugation enriches extracellular vesicles from tissue culture supernatants in small and large scales. Journal of Extracellular Vesicles, 2018, 7, 1528109.	12.2	164
61	Tc toxin activation requires unfolding and refolding of a Î <sup>2</sup> -propeller. Nature, 2018, 563, 209-213.	27.8	45
62	Modulation of septin higher-order structure by the Cdc28 protein kinase. Biologia (Poland), 2018, 73, 1025-1033.	1.5	4
63	Mechanism of loading and translocation of type VI secretion system effector Tse6. Nature Microbiology, 2018, 3, 1142-1152.	13.3	88
64	Reconstitution of a 26-Subunit Human Kinetochore Reveals Cooperative Microtubule Binding by CENP-OPQUR and NDC80. Molecular Cell, 2018, 71, 923-939.e10.	9.7	68
65	Electron cryo-microscopy structure of the canonical TRPC4 ion channel. ELife, 2018, 7, .	6.0	83
66	Single particle cryo-EM — an optimal tool to study cytoskeletal proteins. Current Opinion in Structural Biology, 2018, 52, 16-24.	5.7	11
67	Electron cryomicroscopy as a powerful tool in biomedical research. Journal of Molecular Medicine, 2018, 96, 483-493.	3.9	11
68	Structural transitions of F-actin upon ATP hydrolysis at near-atomic resolution revealed by cryo-EM. Nature Structural and Molecular Biology, 2018, 25, 528-537.	8.2	171
69	Membrane insertion of Î $\pm$ -xenorhabdolysin in near-atomic detail. ELife, 2018, 7, .	6.0	27
70	Retromer-driven membrane tubulation separates endosomal recycling from Rab7/Ypt7-dependent fusion. Molecular Biology of the Cell, 2017, 28, 783-791.	2.1	32
71	Sensory Rhodopsin I and Sensory Rhodopsin <scp>II</scp> Form Trimers of Dimers in Complex with their Cognate Transducers. Photochemistry and Photobiology, 2017, 93, 796-804.	2.5	20
72	Structure of the RZZ complex and molecular basis of its interaction with Spindly. Journal of Cell Biology, 2017, 216, 961-981.	5.2	65

#	Article	IF	CITATIONS
73	Architecture and mechanism of the late endosomal Rab7-like Ypt7 guanine nucleotide exchange factor complex Mon1–Ccz1. Nature Communications, 2017, 8, 14034.	12.8	59
74	The molecular basis of Alzheimer's plaques. Science, 2017, 358, 45-46.	12.6	24
75	Lipid Nanodiscs as a Tool for High-Resolution Structure Determination of Membrane Proteins by Single-Particle Cryo-EM. Methods in Enzymology, 2017, 594, 1-30.	1.0	59
76	Near-atomic structure of jasplakinolide-stabilized malaria parasite F-actin reveals the structural basis of filament instability. Proceedings of the National Academy of Sciences of the United States of America, 2017, 114, 10636-10641.	7.1	64
77	High-resolution Single Particle Analysis from Electron Cryo-microscopy Images Using SPHIRE. Journal of Visualized Experiments, 2017, , .	0.3	161
78	Cryo‣M Revolutionizes the Structure Determination of Biomolecules. Angewandte Chemie - International Edition, 2017, 56, 16450-16452.	13.8	14
79	Eine coole Technik: Kryoelektronenmikroskopie. Nachrichten Aus Der Chemie, 2017, 65, 1086-1088.	0.0	Ο
80	Structural basis for tRNA-dependent cysteine biosynthesis. Nature Communications, 2017, 8, 1521.	12.8	6
81	Electron Cryoâ€microscopy as a Tool for Structureâ€Based Drug Development. Angewandte Chemie - International Edition, 2017, 56, 2846-2860.	13.8	36
82	Kryoâ€Elektronenmikroskopie als Methode für die strukturbasierte Wirkstoffentwicklung. Angewandte Chemie, 2017, 129, 2890-2905.	2.0	10
83	Haptoglobin. Antioxidants and Redox Signaling, 2017, 26, 814-831.	5.4	113
84	Multivalent Rab interactions determine tether-mediated membrane fusion. Molecular Biology of the Cell, 2017, 28, 322-332.	2.1	54
85	Kryoâ€Elektronenmikroskopie revolutioniert die Strukturbestimmung von Biomolekülen. Angewandte Chemie, 2017, 129, 16670-16672.	2.0	2
86	A recombinant BBSome core complex and how it interacts with ciliary cargo. ELife, 2017, 6, .	6.0	69
87	Molecular requirements for the inter-subunit interaction and kinetochore recruitment of SKAP and Astrin. Nature Communications, 2016, 7, 11407.	12.8	31
88	Membrane insertion of a Tc toxin in near-atomic detail. Nature Structural and Molecular Biology, 2016, 23, 884-890.	8.2	88
89	Cryo-EM structure of a human cytoplasmic actomyosin complex at near-atomic resolution. Nature, 2016, 534, 724-728.	27.8	212
90	Insights from the reconstitution of the divergent outer kinetochore of <i>Drosophila melanogaster</i> . Open Biology, 2016, 6, 150236.	3.6	41

#	Article	IF	CITATIONS
91	The mother of all actins?. ELife, 2016, 5, .	6.0	3
92	Condensation Agents Determine the Temperature–Pressure Stability of Fâ€Actin Bundles. Angewandte Chemie - International Edition, 2015, 54, 11088-11092.	13.8	8
93	Deciphering the Tubulin Code. Cell, 2015, 161, 960-961.	28.9	10
94	pHâ€Regulated Selectivity in Supramolecular Polymerizations: Switching between Co―and Homopolymers. Chemistry - A European Journal, 2015, 21, 3304-3309.	3.3	69
95	The Habc Domain of the SNARE Vam3 Interacts with the HOPS Tethering Complex to Facilitate Vacuole Fusion. Journal of Biological Chemistry, 2015, 290, 5405-5413.	3.4	35
96	Functional homologies in vesicle tethering. FEBS Letters, 2015, 589, 2487-2497.	2.8	27
97	The role of Bni5 in the regulation of septin higher-order structure formation. Biological Chemistry, 2015, 396, 1325-1337.	2.5	19
98	An Interbacterial NAD(P)+ Glycohydrolase Toxin Requires Elongation Factor Tu for Delivery to Target Cells. Cell, 2015, 163, 607-619.	28.9	203
99	Determinants of amyloid fibril degradation by the PDZ protease HTRA1. Nature Chemical Biology, 2015, 11, 862-869.	8.0	88
100	Structure of the F-actin–tropomyosin complex. Nature, 2015, 519, 114-117.	27.8	321
101	Structure of Mega-Hemocyanin Reveals Protein Origami in Snails. Structure, 2015, 23, 93-103.	3.3	27
102	Architecture and conformational switch mechanism of the ryanodine receptor. Nature, 2015, 517, 39-43.	27.8	282
103	Exploring the Stability Limits of Actin and Its Suprastructures. Biophysical Journal, 2014, 107, 2982-2992.	0.5	23
104	Structural Identification of the Vps18 β-Propeller Reveals a Critical Role in the HOPS Complex Stability and Function. Journal of Biological Chemistry, 2014, 289, 33503-33512.	3.4	13
105	A Facile Method for Preparation of Tailored Scaffolds for DNAâ€Origami. Small, 2014, 10, 73-77.	10.0	44
106	The Centrosomal Adaptor TACC3 and the Microtubule Polymerase chTOG Interact via Defined C-terminal Subdomains in an Aurora-A Kinase-independent Manner. Journal of Biological Chemistry, 2014, 289, 74-88.	3.4	39
107	Mechanism of Tc toxin action revealed in molecular detail. Nature, 2014, 508, 61-65.	27.8	149
108	Prebiotic Cell Membranes that Survive Extreme Environmental Pressure Conditions. Angewandte Chemie - International Edition, 2014, 53, 8397-8401.	13.8	18

#	Article	IF	CITATIONS
109	Modular Assembly of RWD Domains on the Mis12 Complex Underlies Outer Kinetochore Organization. Molecular Cell, 2014, 53, 591-605.	9.7	116
110	The pseudo GTPase CENP-M drives human kinetochore assembly. ELife, 2014, 3, e02978.	6.0	107
111	Gestalt-Binding of tropomyosin on actin during thin filament activation. Journal of Muscle Research and Cell Motility, 2013, 34, 155-163.	2.0	53
112	Functional Characterization of Human Myosin-18A and Its Interaction with F-actin and GOLPH3. Journal of Biological Chemistry, 2013, 288, 30029-30041.	3.4	52
113	Role of centrosomal adaptor proteins of the TACC family in the regulation of microtubule dynamics during mitotic cell division. Biological Chemistry, 2013, 394, 1411-1423.	2.5	45
114	A syringe-like injection mechanism in Photorhabdus luminescens toxins. Nature, 2013, 495, 520-523.	27.8	130
115	Molecular architecture of the human protein deacetylase Sirt1 and its regulation by AROS and resveratrol. Bioscience Reports, 2013, 33, .	2.4	30
116	FHOD1 is a combined actin filament capping and bundling factor that selectively associates with actin arcs and stress fibers. Journal of Cell Science, 2013, 126, 1891-901.	2.0	74
117	Ras GTPase activating (RasGAP) activity of the dual specificity GAP protein Rasal requires colocalization and C2 domain binding to lipid membranes. Proceedings of the National Academy of Sciences of the United States of America, 2013, 110, 111-116.	7.1	41
118	The role of Cdc42 and Gic1 in the regulation of septin filament formation and dissociation. ELife, 2013, 2, e01085.	6.0	65
119	Molecular architecture of the multisubunit homotypic fusion and vacuole protein sorting (HOPS) tethering complex. Proceedings of the National Academy of Sciences of the United States of America, 2012, 109, 1991-1996.	7.1	227
120	Real-space processing of helical filaments in SPARX. Journal of Structural Biology, 2012, 177, 302-313.	2.8	31
121	Structure of the Rigor Actin-Tropomyosin-Myosin Complex. Cell, 2012, 150, 327-338.	28.9	297
122	Membrane Fusion Intermediates via Directional and Full Assembly of the SNARE Complex. Science, 2012, 336, 1581-1584.	12.6	210
123	Tropomyosin Movement on F-actin Analyzed by Energy Landscape Determination. Biophysical Journal, 2012, 102, 17a.	0.5	1
124	Functional characterization of the human α-cardiac actin mutations Y166C and M305L involved in hypertrophic cardiomyopathy. Cellular and Molecular Life Sciences, 2012, 69, 3457-3479.	5.4	52
125	Structural Characterization of Polyglutamine Fibrils by Solid-State NMR Spectroscopy. Journal of Molecular Biology, 2011, 412, 121-136.	4.2	88
126	The Fas–FADD death domain complex structure reveals the basis of DISC assembly and disease mutations. Nature Structural and Molecular Biology, 2010, 17, 1324-1329.	8.2	236

#	Article	IF	CITATIONS
127	Rubisco in complex with Rubisco large subunit methyltransferase. Proceedings of the National Academy of Sciences of the United States of America, 2009, 106, 3160-3165.	7.1	27
128	STIM1 Clusters and Activates CRAC Channels via Direct Binding of a Cytosolic Domain to Orai1. Cell, 2009, 136, 876-890.	28.9	839
129	Oligomeric Structure and Functional Characterization of the Urea Transporter from Actinobacillus pleuropneumoniae. Journal of Molecular Biology, 2009, 387, 619-627.	4.2	22
130	Electron Crystallography as a Technique to Study the Structure on Membrane Proteins in a Lipidic Environment. Annual Review of Biophysics, 2009, 38, 89-105.	10.0	66
131	Death Domain Assembly Mechanism Revealed by Crystal Structure of theÂOligomeric PIDDosome Core Complex. Cell, 2007, 128, 533-546.	28.9	244
132	Structure of ClnK1 with bound effectors indicates regulatory mechanism for ammonia uptake. EMBO Journal, 2007, 26, 589-599.	7.8	57
133	Revival of electron crystallography. Current Opinion in Structural Biology, 2007, 17, 389-395.	5.7	48
134	Structural Insight into Pre-B Cell Receptor Function. Science, 2007, 316, 291-294.	12.6	101
135	A Virulence Locus of Pseudomonas aeruginosa Encodes a Protein Secretion Apparatus. Science, 2006, 312, 1526-1530.	12.6	984
136	Heterologously Expressed GLT-1 Associates in â^¼200-nm Protein-Lipid Islands. Biophysical Journal, 2006, 91, 3718-3726.	0.5	15
137	Structure and Function of Prokaryotic Glutamate Transporters fromEscherichia coli and Pyrococcus horikoshiiâ€. Biochemistry, 2006, 45, 12796-12805.	2.5	35
138	The Architecture of the Multisubunit TRAPP I Complex Suggests a Model for Vesicle Tethering. Cell, 2006, 127, 817-830.	28.9	166
139	Assembly of the Major Light-harvesting Chlorophyll-a/b Complex. Journal of Biological Chemistry, 2006, 281, 25156-25166.	3.4	26
140	Oligomeric Structure of the Carnitine Transporter CaiT from Escherichia coli. Journal of Biological Chemistry, 2006, 281, 4795-4801.	3.4	30
141	High-yield Expression, Reconstitution and Structure of the Recombinant, Fully Functional Glutamate Transporter GLT-1 from Rattus norvegicus. Journal of Molecular Biology, 2005, 351, 598-613.	4.2	25
142	Accelerated 2D Classification With ISAC Using GPUs. Frontiers in Molecular Biosciences, 0, 9, .	3.5	4